# The effects of severe hypoxia on glycolytic flux and enzyme activity in solid tumour models

**Hannah Smith[1], Mary Board[1], Andrea Pellagatti[1,2], Helen Turley[1], Jacqueline Boultwood[1,2] & Richard Callaghan[1,3]**

[1]Nuffield Department of Clinical Laboratory Sciences, John Radcliffe Hospital, The University of Oxford, Headington, UK

[2]NIHR Biomedical Research Centre, Oxford, UK

[3]Division of Biomedical Science & Biochemistry, Research School of Biology, The Australian National University Canberra, ACT 0200, Australia

Running Title: *Effects of anoxia on glycolysis in cancer*

To whom correspondence should be addressed: Richard Callaghan, Biomedical Science & Biochemistry, Research School of Biology, Building 134, Linnaeus Way, The Australian National University Canberra, ACT 0200, Australia, Tel - +61 6125 0824; E-mail; richard.callaghan@anu.edu.au

**Keywords;** glycolysis; tumour cell biology; tumour spheroid; hypoxia; anoxia; Hif1; Warburg effect; glucose metabolism; glutamine metabolism; pentose-phosphate pathway

**Background:** Severe hypoxia is prevalent in solid tumours and necessitates compensatory changes to nutrient metabolism.
**Results:** Under severe hypoxia tumour models ensured sufficient ATP production and cell viability.
**Conclusion:** Maintaining ATP production diverted glucose and its metabolites from biosynthesis.
**Significance:** Greater understanding of tumour cells under severe hypoxia may provide novel therapeutic targets in this recalcitrant population.

## ABSTRACT

Solid tumours contend with, and adapt to, a hostile micro-environment that includes limited availability of nutrient fuels and oxygen. The presence of hypoxia ($O_2$ < 5%) stabilises the transcription factor Hif1 and results in numerous cellular adaptations including increased flux of glucose through glycolysis. Increasingly more sophisticated analysis of tumour oxygenation has revealed large gradients of oxygen tension and significant regions under severe hypoxia ($O_2$ < 1%). The present investigation has demonstrated a significant increase in the glycolytic flux rate when tumour spheroids were exposed to 0.1% $O_2$. The severe hypoxia was associated with uniform pimonidazole adduct formation and elevated levels of Hif1α and c-Myc. This resulted in elevated expression of GLUT and MCT transporters, in addition to increased activity of PFK1 in comparison to that observed in normoxia. However, the protein expression and enzymatic capacity of HK2, G6PDH, PK and LDH were all reduced by severe hypoxia. Clearly the effects of exposure to severe hypoxia lead to a significantly abridged Hif1 response, yet one still able to elevate glycolytic flux and prevent loss of intermediates to anabolism.

Cancer cells adopt a distinct metabolic profile from healthy tissues; in particular they display a heavy reliance on the contribution of glycolysis to meet energy demands (1). Even in the presence of sufficient oxygen and fully functional mitochondria, cancer cells

preferentially utilise the "aerobic glycolysis" route. This switch from oxidative phosphorylation (36 ATP per glucose) to glycolysis (2 ATP per glucose) appears at odds with the demands of highly proliferative tissue. Flux through oxidative phosphorylation is not negligible (2), but the balance compared to glycolysis is reduced. Glucose uptake into cancer cells is sufficiently high to ensure a high flux through glycolysis; however, the passage of pyruvate towards the TCA cycle via acetyl-CoA is depressed (3,4). This situation will enable diversion of intermediates to anabolic pathways to generate glycerol for complex lipid synthesis, NADPH for biosynthetic reductions and ribose sugars for nucleotides in DNA and RNA. Clearly, cancer cells have adapted their metabolic strategy to maintain a balance between energy provision and biomass production.

The molecular basis for the switch in metabolic profile of cancer cells involves the input of several transcription factors and tumour suppressor genes. For example, expression of the transcription factor c-Myc is increased in approximately 70% of human cancers (5) and it regulates 15% of human genes, many of which are associated with metabolism (6). Expression of glucose transporters and the LDH enzyme are key targets for c-Myc to ensure elevated glycolytic flux (7-9). In addition, most of the enzymes involved in glycolysis display a c-Myc binding site within their gene sequence (5,10). The tumour suppressor, p53, normally represses transcriptional activity for several GLUT isoforms (11). However, it is highly mutated in most cancers and the repression of glucose transporter expression is removed.

Pyruvate kinase (PK) catalyses the final reaction of glycolysis and the M1 isoform dominates in healthy tissues forming an active tetrameric assembly. In tumour cells the M2 isoform is over-expressed (12) and may form an active tetrameric, or a less-active dimeric assembly (13). The presence of dimeric PK-M2 reduces the rate of pyruvate formation and results in elevated levels of glycolytic intermediates. As a consequence, a proportion of the intermediates will enter anabolic pathways to produce lipid, nucleotides and amino-acids.

It is clear that cancer cell metabolism has adapted to its specific requirements through the actions of multiple regulatory factors. In particular, transcription factors, allosteric intermediates and tumour suppressor genes combine to increase flux of glucose into glycolysis and stimulate the activities of glycolytic enzymes.

The uncontrolled growth of tumours requires sufficient supply of metabolic nutrients and the disorganised architecture of solid tumours prevents uniform and abundant nutrient supply to all cells. Consequently, gradients of nutrients and oxygen occur and it was estimated in 1919 that oxygenation of cells in a tumour would only occur to a maximal distance of 150μm from a capillary (14) and experimental studies have suggested a diffusion limit of 235μm (15). More recent experimental evidence has demonstrated steep gradients of oxygen partial pressure that fall to near zero levels at cells distant from vessels (16,17). The crisis in oxygen availability engenders numerous adaptive responses in tumours and of primary importance is angiogenesis to alleviate the supply issues. However, the angiogenic vessels are frequently poorly formed, leaky and do not evenly distribute through the tumour mass. The high interstitial and hydrostatic pressures also prevent homogeneous distribution of nutrients and oxygen (18,19). In addition, the clearance of metabolic waste products from deeper regions of tumours is also severely limited. Therefore, a large cohort of cells in solid tumours is poorly oxygenated, has limited supply of metabolic nutrients and this may lead to regions of necrosis.

The cellular response to hypoxia combats some of these issues and ensures adequate provision of energy and biosynthetic precursors. Hypoxia-inducible factor (Hif) is a major transcription factor that co-ordinates the cellular response to low oxygen (10,20). In hypoxia, Hif1α escapes proteosomal degradation (21), the heterodimer with Hif1β is stabilised, and results in transcriptional activation of target genes (10). Hif1 targets genes involved in numerous cellular functions (e.g. apoptosis, DNA repair, lipid metabolism) and a number are specifically related to glucose metabolism.

Hif1 induces expression of pyruvate dehydrogenase kinase 1 (PDK1) which phosphorylates, and thereby inactivates, the PDH enzyme. PDH catalyses the conversion of

pyruvate to acetyl-CoA and a reduction in its activity will lower entry of carbon fuel derived from glucose into the TCA cycle. Hif1 has also been demonstrated to increase expression of PKM2 (22), LDH-A and several GLUT isoforms. The combined effect of these alterations to protein expression or activity is to elevate flux into the glycolytic pathway and direct the product pyruvate to lactate; thereby avoiding entry to the TCA cycle for complete oxidation. The activation of Hif1 has also been reported to increase expression of HK2, enolase, GAPDH, PFK-L and TPI in cancer cell lines and clinical samples (20,23,24). Overall, Hif1 mediates the activation of most steps in the glycolytic pathway.

Is there a correlation between the extent of hypoxia and the degree to which glycolytic flux is stimulated? Hypoxia can be broadly defined as conditions where the partial pressure of oxygen drops below 10mm Hg (~1.4%) (25). The $O_2$ partial pressure is in air is 150mm Hg (~20%) and 100mm Hg in arterial blood. Healthy tissues display considerable variability, with partial pressures of oxygen in liver and kidney at 20 and 70mm Hg respectively. Considerable effort has been placed into documenting the degree of oxygenation in most types of cancer. Pancreatic cancer has a median oxygen partial pressure of 2mm Hg, compared to 52mm Hg in non-cancerous tissue (26). Moreover, the fraction of pancreatic cancer tissue mass with an oxygen partial pressure of <2.5mm Hg was 20%. Head and neck cancers have been reported to display median oxygen partial pressures of 3-9mm Hg with a range of 0-59mm Hg reported (27,28). Head and neck cancers have also been shown to contain 22% of their mass at $O_2$ partial pressure <2.5mm Hg. Prostate cancer has a mean oxygen partial pressure of 9.5mm Hg with a median of 6.1mm Hg and 70% of the tumour is found in an environment with <10mm Hg (29). Hypoxia is omnipresent in solid tumours and the degree of hypoxia correlates inversely with patient prognosis. Moreover, it is the fraction of hypoxic cells in a tumour that correlate with outcome or prognosis.

A great deal of research has focussed on hypoxia in the range 5-10mm Hg and the effects on glycolysis and nutrient utilisation are well-documented. Comparatively, little information is available under conditions of severe hypoxia. Given the small sample of statistics presented above, the focus on 5-10mm Hg level hypoxia may not represent the extent of cellular alterations of a significant proportion of tissue. In the present investigation the effects of severe hypoxia (1.4mmHg) on glycolytic flux were investigated in a solid tumour model. Expression and the activities of key enzymes or transporters associated with glucose and glutamine utilisation were measured in solid tumour models. The data demonstrate that cellular adaptation to a severe hypoxic environment is distinct from that observed at lower degrees of hypoxia.

## MATERIALS AND METHODS

### *Materials*

RPMI-1640 medium, foetal bovine serum and trypsin with EDTA were purchased from Invitrogen (Paisley, UK). The penicillin and streptomycin was from Lonza (Wokingham, UK). AnaeroGen sachets and Anaerobic indicator were from Fisher Scientific (UK). Protease inhibitors and glutamate pyruvate transaminase were from Roche (Mannheim, Germany). The DC detergent compatible protein assay and Kaleidoscope Precision Plus protein standards were from Bio Rad Laboratories (Hercules, USA). The reduced and oxidised forms of β-Nicotinamide-adenine dinucleotide ($NADP^+$) and β-Nicotinamide-Adenine Dinucleotide Phosphate ($NAD^+$), Glucose-6-phosphate Dehydrogenase, Hexokinase, and NAD Lithium Salt were from Calbiochem – Merck Ltd (Nottingham, UK). EZ-Chemiluminescence Detection kit for HRP was from Geneflow Ltd. Primary antibodies to GLUT1, GLUT3, MCT1, MCT4, p27 and c-Myc antibody HRP (all raised in rabbit) were purchased from Santa Cruz biotechnology Inc (USA). Primary antibodies to Glucose 6 phosphate dehydrogenase, glutamate dehydrogenase, pyruvate kinase (HRP) and lactate dehydrogenase (HRP) as well as secondary anti rabbit and anti-goat antibodies conjugated to HRP were from Abcam UK. The primary antibody to HIF-1α (Clone 54) was from Becton Dickinson UK Ltd. Primary antibodies to PFKP, hexokinase II and ASCT2 were from New England Biolabs (Herts, UK). Primary antibodies to PFKL and PFKM were from Sigma-Aldrich. (Dorset, UK). The primary antibody to the Ki-67 antigen (MIB-1) and the polyclonal goat anti mouse HRP secondary antibody were from Dako UK (Ely, UK). The primary antibody to pimonidazole was included

in a kit from Chemicon International Inc (USA). Normal horse serum and universal anti-mouse anti-rabbit secondary antibody for IHC was from Vector Laboratories Inc (California, USA). The Novolink polymer detection system was from Leica biosystems. D-[5-$^{3}$H(N)]-glucose was from PerkinElmer.

***Production of tumour spheroids from DLD1 cells***

DLD1 human colon adenocarcinoma cells were primarily grown as monolayers in RPMI-1640 medium as previously described (30). Tumour spheroids (TS) were grown as suspension cultures from a seeding density of 2.5 x $10^5$ cells $ml^{-1}$ in 20 ml and stirred at 55 rpm (Techne MCS-104S) (37°C, 5% $CO_2$), allowing spheroids to form, as described (31). TS diameter was used as a measure of growth and diameters of at least 20 TS in a 1 ml fraction were measured using a graduated calibrated microscope eyepiece graticule. TS between 200-400μm in diameter were used for metabolic analyses. This was typically at day 2 of TS growth where TS had an average diameter of 232±7μm (n=200 TS).

To prepare homogenates, the TS were collected by gravity sedimentation, the growth medium discarded, and the TS were re-suspended in homogenisation buffer (0.05M Tris-HCl (pH 8.0)) containing protease inhibitors. The TS were homogenized extensively using a glass homogenizer and aliquots (50μl) stored at -80°C. Protein concentration of TS homogenates was determined using the DC Brad (BioRad) protein assay according to the manufacture's protocol.

***Growth of tumour spheroids in severe hypoxia***

DLD1 TS with a 200-400μm diameter were transferred in 100μl medium to a 96 well plate, containing a base coat of 0.75% (w/v) agarose in serum-free medium. The plate was placed in a 3.5L anaerobic chamber, which was incubated for 16 hours at 37°C. An AnaeroGen sachet, containing ascorbic acid and activated carbon to absorb the oxygen in the chamber and produce carbon dioxide, was placed inside the chamber (32). Hypoxic conditions were confirmed with an anaerobic indicator strip, a cotton strip containing the redox indicator resazurin that undergoes a colour change from white to red on exposure to oxygen.

The viability of $TS^H$ compared to $TS^N$ was assayed by measuring the amount of cellular outgrowth from the spheroid following hypoxic exposure. After hypoxic incubation tumour spheroids were transferred to an uncoated 96-well tissue culture plate and incubated for 72h to allow cellular outgrowth from the tissue (30). Following outgrowth, the medium was aspirated and replaced with 5g $L^{-1}$ methylene blue in 50% (v/v) methanol to fix and stain the cells. The wells were washed three times in PBS and the radial outgrowth measured using a graduated microscope eye-piece graticule. The radius of the tumour spheroids was subtracted from the measurements and the degree of outgrowth was expressed as a fraction of spheroid size.

***Immunohistochemistry of tumour spheroids***

TS were fixed, embedded and cut into 5μm sections as previously described (Mellor BP 2005). To enable detection of specific proteins, antigen retrieval was done by incubating slides in 50mM Tris/200mM EDTA buffer, (pH 9) in a Decloaking chamber (Biocare Medical) (25p.s.i for 2 minutes). Slides were blocked with normal 2.5%(v/v) horse serum prior to incubation with primary monoclonal antibody to Ki67 (1:100) or $p27^{Kip1}$ (1:150), for 1 hour at room temperature. Bound Ki67 antibody was detected using an anti-mouse secondary whilst $p27^{Kip1}$ bound antibody was detected using a Novolink polymer kit. To determine their oxygenation status, TS were cultured with 100μM pimonidazole in the medium for the final 16 hours of growth. Slides were also blocked with normal horse serum prior to incubation with the primary monoclonal mouse anti-human antibody (1:100) for 1 hour at room temperature. Bound antibody was detected using a universal anti-mouse secondary antibody. Detection for all three targets was achieved using DAB substrate chromogen and hematoxylin counterstain.

***Metabolic enzyme activity in tumour spheroids***

The activities of enzymes catalysing the key reactions in energy generating pathways were measured in the TS homogenates using spectrophotometric assays (Hitachi Model U-2010 spectrometer). Full details of the assays[1] and their optimisation to tumour spheroids have been previously described (33,34). Reactions were monitored by continuous recording of the change in absorbance at λ=340nm due to the reduction or oxidation of NAD(P)H or $NAD(P)^+$ either within a single reaction or a coupled

[1] *Details in Supplementary Table S1*

reaction system. Enzyme specific activity was then calculated from the initial rate of change of absorbance using the Beer Lambert law.

***Expression levels of enzymes in tumour spheroids***

TS homogenates were mixed with reducing Laemmli sample buffer and heated at 95ºC for 10 minutes. Total protein was separated by SDS PAGE electrophoresis and then transferred to a nitrocellulose membrane. The membrane was blocked overnight at 4ºC or at room temperature for 1-2 hours with 5% skim-milk or BSA (w/v) in PBS-T. The enzymes of interest were detected according to the antibody conditions[2] provided by the manufacturers, in most cases the secondary antibody was conjugated to HRP. Nitrocellulose membranes were washed twice for 10 mins in PBS supplemented with 0.1% (v/v) Tween20 (PBS-T) and immuno-reactivity measured with the EZ-Chemiluminescence Detection kit.

***Measurement of glycolytic flux***

Glycolytic flux in TS of 200-400μm diameter was determined by measuring the rate of tritium removal from D-[5-$^3$H(N)]-glucose (35). TS were washed twice and re-suspended in 5ml sterile PBS, the solution was mixed well before transferring 0.5ml to each of 6 wells in an uncoated 24 well plate. Each well was supplemented with 0.5ml growth medium containing 10mM glucose. After a 30-minute incubation, 0.5 ml of medium supplemented with 0.04miCi/mM [D-[5-$^3$H(N)]-glucose was added and the TS were incubated for 16 hours under normoxic or hypoxic conditions. Following the incubation, medium was removed and snap frozen at -20°C. The $^3H_2O$ produced was separated from labelled D-[5-$^3$H(N)]-glucose in the samples by column chromatography using a DOWEX-borate column. Carbohydrates in the sample bind to borate in the stationary phase of the column and the $^3H_2O$ in the sample was eluted with 2ml of water. The radioactivity in the water eluate was measured by scintillation counting. All values were normalised to protein content measured from control wells.

***Gene expression profiling***

RNA was extracted from tumour spheroids using TRIZOL. For each sample, 100ng of total RNA was amplified and labelled with the 3' IVT Express Kit following the manufacturer's protocol (Affymetrix, Santa Clara USA). Biotin-labelled fragmented cRNA (10μg) was hybridised to GeneChip Human Genome U133 Plus2.0 Arrays (Affymetrix), which covers more than 47,000 transcripts representing 39,000 human genes. Hybridisation occurred at 45ºC for 16 hr in a Hybridisation Oven (Affymetrix). Chips were then washed and stained in a Fluidics Station 450 (Affymetrix) and scanned with a GeneChip Scanner (Affymetrix). Data was analysed using GeneSpring 7.3.1 software (Agilent) as previously described (36).

***Data analysis***

Enzyme assays were analysed using linear regression analysis of the raw spectrophotometric data to give reaction rates. Enzyme activity was then calculated according to the Beer Lambert law, and corrected for total protein concentration.

Western blots were analysed by densitometry using Image J. The raw data was normalised to give expression levels relative to the mean densitometry observed in $TS^N$ on each western blot. Initial investigations showed that β-actin levels were not consistent between the three micro-environmental conditions utilized in this study. This is consistent with studies by Farmer et al who determined that changes in cell growth conditions may alter actin synthesis (37). Therefore in this study sample loading was controlled by using specific amounts of total protein.

Enzymatic and expression data were compared using one-way ANOVA with the Bonferroni's multiple comparison post-hoc test. All regression analysis and statistical comparisons were done using GraphPad Prism 4.

## RESULTS

***The 3-D solid tumour model for severe hypoxia***

The 3-D tumour spheroid (TS) model has been widely used to investigate cancer biology and the efficacy of treatment regimes. TS from the DLD1 cell line were grown to a diameter of 200-400μm for the present investigation, although they can grow to diameters in excess of 1000μm. However, those above 500μm display considerable heterogeneity of cell populations

[2] *See also Supplementary Table S2*

and nutrient/$O_2$ gradients (33,38). Figure 1a provides a cross-section of TS grown under standard normoxic conditions ($TS^N$) and Figure 1c shows TS stained for the marker of proliferating cells, Ki67. The presence of cells expressing Ki67 was observed throughout the tissue mass. Figure 1e shows the protein expression pattern for the marker of quiescence p27. The degree of staining was less intense than observed for Ki67 and did not display any specific localisation in $TS^N$.

It has also been estimated that the diffusion limit for $O_2$ in solid tumours is approximately 200μm, thereby providing further justification for using TS with $\phi \leq 400\mu m$. This investigation provides comparison between TS grown under conditions of normoxia and severe hypoxia. Therefore, the absence of measurable hypoxia in the control (i.e. $TS^N$) tissue was essential. Tumour spheroids were grown under hypoxic conditions ($TS^H$) using an anaerobic jar containing sachets with activated carbon and ascorbic acid to generate an atmosphere of <1% $O_2$. $O_2$ levels had been demonstrated to drop from 20% to 0.1% within 45 minutes and remained stable for at least 24 hours (31).

The TS were grown under these conditions for 16 hours and the degree of hypoxia determined by measuring the presence of pimonidazole. Figure 1 (a-b) provides a comparison of the presence of pimonidazole adducts between TS grown under normoxic and hypoxic conditions. The $TS^H$ demonstrated extensive pimonidazole staining, which was observed throughout the tissue. In contrast, the $TS^N$ displayed negligible levels of pimonidazole adduct staining in the tissue. The effects of hypoxic incubation were also examined on the proliferative capacity of the TS in order to provide a measure of tissue viability. The growth under severe hypoxic conditions for 16 hours did not alter the protein expression levels or pattern for the markers of proliferation (Ki67 – Figure 1c-d) or quiescence (p27 – Figure 1e-f). The retention of proliferative capacity suggests that the treatment did not alter the cell viability within the tissue.

Further validation of the integrity, or viability, of the $TS^H$ was assessed using the cellular outgrowth assay. Following the hypoxic incubation, TS were placed in cell culture plates for a 72 hour recovery period. Once the TS adhered to the plate, the viable outer rim cells proliferate and grow in a radial manner from the spheroid, as shown in Figure 2a. The degree of radial outgrowth from the dark central TS mass ($R_{tot} - R_{TS}$) is a measure of proliferative capacity and therefore of the cell viability. As shown in Figure 2b, there was no statistically significant difference in the radial outgrowth between the two growth conditions, thereby indicating that following hypoxic incubation, the $TS^H$ contained viable cells.

Cancer cells undergo considerable adaptation to ensure survival under conditions of hypoxia and the response involves the major transcription factor Hif-1. Stabilisation of the Hif-1 transcription factor affects genes involved in angiogenesis, survival, pH regulation and metabolism to name a few. In particular, expression of the Hif1α protein subunit is stabilised under conditions of oxygen deprivation. Figure 3 shows a representative western blot for the expression of Hif1α protein (132kDa) in TS grown under conditions of normoxia and severe hypoxia for 16 hours. The histogram summarises multiple observations and reveals a statistically significant ($P<0.001$), 3.3 fold increase in the level of Hif1α protein in $TS^H$ compared to the normoxic control.

The transcription factor c-Myc is a driver for proliferation, growth and metabolism in cancer cells, often with constitutive expression. Increased levels of c-Myc have been shown to modulate the expression of several transporters and enzymes associated with glucose catabolism and glutamine utilisation. Moreover, there are several reports of a relationship between c-Myc and Hif1α in cancer cells, presumably involving the response to hypoxia (39). The representative western blot in Figure 3 demonstrates that c-Myc expression was also increased in TS grown under severe hypoxia. In fact, data from multiple observations revealed that 16hr incubation at 0.1% $O_2$ resulted in a statistically significant two-fold increase in c-Myc expression.

The use of TS with diameters of 200-400μm generates a homogeneous cellular distribution in TS. Moreover, the growth of TS at $O_2$ tension of 0.1% generates TS with clear evidence of hypoxia, yet retention of cell viability. The latter was assessed by two measures of proliferative capacity, which is a stringent measure of overall cell function. Finally, expression the transcription factors c-Myc and Hif1α, which

regulate numerous metabolic pathways, are significantly increased by severe hypoxia.

***Metabolic alterations due to severe hypoxia in a 3-D tumour model***

The TS model was subsequently used to investigate the effects of severe hypoxia on the utilisation of glucose and glutamine. In particular, overall glycolytic flux was assessed and the contributions of key metabolic enzymes and transporters were described. The use of TS with $\phi \leq 400\mu m$ ensured adequate availability of nutrients and oxygen, thereby reducing supply issues as a factor in metabolic assessment. Homogenates of TS were used to determine the activities and expression levels of enzymes. Relative protein expression was estimated using western blot analysis[3] and the data quantitated using densitometry, which is summarised in the tables below.

Glycolytic flux was measured to provide an indication of catabolism in TS grown under normoxia and severe hypoxia. The glycolytic flux rate was measured by the release of $^3H_2O$ following the inclusion of 5-[$^3$H]-glucose in the growth medium. The $^3H_2O$ is released in the penultimate reaction of glycolysis (2-phospho-glycerate → phospho-enol-pyruvate), which is catalysed by enolase. Under conditions replete with glucose (11mM) and normoxia (20% $O_2$), the glycolytic flux rate was 19.3±1.7 nmol $min^{-1}$ $mg^{-1}$ (Table 1). Under severe hypoxia (0.1% $O_2$) the rate of glycolysis was increased by 2-fold to 37.8±3.2 nmol $min^{-1}$ $mg^{-1}$ ($P<0.001$) over a 16-hour period.

The elevated flux rate for glucose through the glycolytic pathway is commensurate with the increased expression of Hif1α and c-Myc proteins. The effects of increased levels of these transcription factors under hypoxia (1-5% $O_2$) typically results in elevated expression of selected, key glycolytic enzymes and nutrient transporters. Protein expression of the glucose transporter GLUT1 was marginally increased under severe hypoxia and levels of the GLUT3 isoform were raised by almost two-fold (Table 2). Both transporters have high affinity for glucose ($K_M$~1mM) and hypoxia response elements in their gene promotor regions. The high glucose concentration of RPMI-1640 medium (11mM) ensured that the transporters were saturated and the uptake of glucose was proportional to their expression.

The activities of several metabolic enzymes were measured (Table 3) under conditions that ensured that the enzyme operated at maximal activity ($V_{MAX}$). This reported activity is a reflection of the maximal capacity for the enzyme at the protein expression levels found in the homogenate. The maximal activity of PFK1 in normoxic conditions was 29±10 nmol $min^{-1}$ $mg^{-1}$, which was not significantly different to the overall glycolytic flux rate (Table 1). This indicates that this enzyme reflects the capacity for glycolysis in these cells and has been thought to dictate the pace of glycolysis.

When TS were grown under severe hypoxia, protein expression of the PFK1-P isoform was unchanged, whereas expression of the PFK1-M and PFK1-L isoforms was significantly reduced (Table 3). The overall capacity of the reaction catalysed by PFK1 was unaffected by severe hypoxia. Moreover, the capacity (32±7 nmol $min^{-1}$ $mg^{-1}$) was also not significantly different to the rate of glycolytic flux (Table 1) under identical growth conditions. This suggests that the glycolytic pathway was operating at the maximal possible rate in severe hypoxia and there was no further capability to respond to conditions of increased ATP demand.

Hexokinase is a near ubiquitously expressed enzyme that phosphorylates glucose in the cytoplasm to facilitate the maintenance of a concentration gradient into cells. The isoforms I-III have high affinity for glucose (i.e. $K_M$<1mM), thereby ensuring saturation of activity in the conditions used for TS growth in this investigation. In TS grown under severe hypoxia the hexokinase activity in the homogenates was reduced from 6.3±1.0 nmol $min^{-1}$ $mg^{-1}$ in normoxia by almost five-fold to a rate of 1.3±0.3 nmol $min^{-1}$ $mg^{-1}$ ($P<0.01$) (Table 3). The drop in activity was associated with a similar 5.9-fold reduction in the protein expression level for the Hexokinase II isoform known to be expressed in cancer cells (Table 3).

The final reaction in glycolysis involves the transfer of a phosphate-group from phospho-enol-pyruvate to ADP. The reaction is catalysed by pyruvate kinase and the reaction leads to the formation of ATP and pyruvate. Overall protein expression of pyruvate kinase was reduced four-fold ($P<0.01$) in TS grown under severe hypoxia

[3] *Representative blots in Supplementary Figure S1*

(Table 3). There was a concomitant reduction in the pyruvate kinase activity of homogenates grown under severe hypoxia to 25% of the activity ($P<0.05$) observed in normoxic conditions (Table 3). This complements previous observations that a switch to the PK-M2 isoform correlates with growth rates in tumours, allowing the funnelling of glycolytic intermediates into biosynthetic pathways (40). The TS of the present investigation appear to divert resources from growth promoting pathways, yet maintain sufficient ATP production from glycolysis.

In tumour cells the immediate fate of pyruvate is primarily the conversion to lactate in conjunction with the oxidation of NADH to $NAD^+$. The liberation of the latter enables continued glycolysis, particularly where flux through oxidative phosphorylation is impaired (e.g. hypoxia). In cancer cells, expression of the LDH-A isoform is under the control of both Hif1α and c-Myc. Despite this, protein expression levels for LDH-A were reduced to 29% of the amount observed in TS grown under normoxic conditions (Table 3). Once again, this reduced protein expression was mirrored by the reduction of the maximal capacity of LDH activity in $TS^H$ homogenates to 384±154 nmol $min^{-1}$ $mg^{-1}$, which is 29% of the activity in $TS^N$ ($P<0.05$).

Expression of the monocarboxylate transporter MCT4 protein isoform was subjected to a modest 1.5-fold increase ($P<0.01$) in $TS^H$ (Table 2). The MCT4 isoform can mediate the efflux of lactate from the cytoplasm and its expression is crucial to maintain pH-homeostasis in cancer cells due to the high glycolytic flux. The elevated expression under severe hypoxia is commensurate with the increased flux rate through glycolysis (Table 1). The related MCT1 isoform is also capable of transporting lactate, pyruvate, ketone bodies and oxo-acids from branch-chain amino-acids. The directionality of lactate flux is dependent on the cellular conditions, but efflux or influx is possible. Expression of MCT1 protein was also increased by approximately 50% ($P<0.01$) when TS were grown under hypoxic conditions (Table 2).

It is possible that TS under severe hypoxia are utilising alternative fuels such as glutamine, which is found at 2mM concentration in RPMI-1640 medium. Table 2 demonstrates that expression of the glutamine (and neutral amino-acid) transporter protein ASCT2 was not significantly altered by severe hypoxia, which is distinct from the elevated glucose uptake observed. Glutamate dehydrogenase (GLDH) is a key enzyme in the process of glutaminolysis, which serves to provide energy and anabolic intermediates from the utilisation of glutamine. The enzyme is highly regulated and catalyses the oxidative deamination of glutamate to produce α-keto-glutarate, NADPH and the liberation of $NH_4^+$. Severe hypoxia did not produce a statistically significant change in the protein expression levels of GLDH in TS (Table 3). However, the activity of GLDH was reduced by five-fold ($P<0.05$) in TS grown under severe hypoxia (Table 3), which is similar to the effects seen for several key glycolytic enzymes.

Another fate for glucose in tumour cells is the pentose phosphate pathway, which provides ribose sugars for nucleotide synthesis and the reduced co-factor NADPH. The latter is used in anabolic pathways and for regeneration of the cellular anti-oxidant GSH. The pathway has a major role in highly proliferative tissue for biomass production. As shown in Table 3, the exposure of TS to a severely hypoxic environment was associated with a dramatic 10-fold reduction in the expression of glucose-6-phosphate dehydrogenase (G6PDH) protein. G6PDH catalyses the oxidation of glucose-6-phosphate to 6-phosphono-glucono-lactone, with the production of NADPH and it constitutes the entry reaction to the PPP. Similarly, the activity of G6PDH was reduced from 23±2 nmol $min^{-1}$ $mg^{-1}$ to 4±3 nmol $min^{-1}$ $mg^{-1}$, which is a statistically significant ($P<0.05$) 5.2-fold reduction.

In summary, the nature of metabolic changes associated with glycolysis under conditions of severe hypoxia is somewhat incongruous. Severe hypoxia was associated with higher glycolytic flux and this was supported by (i) increased expression of glucose transporter proteins to ensure substrate supply, (ii) high metabolic capacity of the key enzyme PFK1, and, (iii) increased expression of transport proteins to clear lactate from the cytoplasm. However, the protein expression levels and maximal capacity of three key enzymes associated with glycolysis were severely depressed. In addition, protein expression levels were frequently at odds with the elevated mRNA levels (Tables 2-3). Elevated mRNA for glycolytic enzymes is a fundamental

outcome of the Hif1α/c-Myc signal. This indicates that the hypoxic response remains intact; namely to cause ↑glycolytic flux. However, it did not ultimately achieve this through a generic increase in expression of enzymes and transporters

## DISCUSSION

The hostile intra-tumour microenvironment requires considerable adaptation to sustain tumour viability and a key driving force for adaptive changes is the presence of hypoxia. The extent of hypoxia varies markedly for tumours and the presence of near total anoxia have been observed in vivo and in clinical samples (26-29). The present investigation focussed on the effects of severe hypoxia on the catabolism of glucose. A TS model system was adopted over simple monolayer systems to more accurately reflect the gradients of nutrients, pH, oxygen and metabolic waste products observed in vivo (41). However, TS sizes were limited to a $\phi$<400μm to maximise the diffusion of oxygen through the tissue. It has been reported that the experimentally derived oxygen diffusion limit is approximately 230μm (15) and that TS $\phi$>400μm exhibit heterogeneous cell populations (33,38). This ensures that the normoxic TS used in this investigation were free of regions containing hypoxic or non-proliferating cells.

TS grown under conditions of severe hypoxia (0.1% $O_2$ or 1.4mm Hg) displayed extensive and homogeneous pimonidazole adduct formation. Moreover, the $TS^H$ reflected the hallmark characteristics of stabilised Hif1α and elevated c-Myc transcription factor expression. These features combined to produce the anticipated increase in flux of glucose through the catabolic glycolytic pathway that has been widely observed in hypoxia (5,10,20). Typically, the elevated glycolytic flux occurs due to the increased expression of several enzymes and transporters associated with the pathway. Under severe hypoxia, mRNA levels were increased for several glycolytic enzymes in response to stabilisation of the transcription factor Hif1α. However, there was an apparent disconnect between the elevated mRNA and the protein expression levels in the $TS^H$. Clearly, the cellular alterations to enzymes associated with glycolysis under conditions of severe hypoxia differ from those adopted at "standard experimental hypoxia" (10-15mm Hg), although the increase in flux was maintained.

As discussed earlier, the stabilisation of Hif1α has been shown to cause a generic increase in transcript and protein levels for glycolytic enzymes to ensure sufficient flux through the pathway. In fact, it has been demonstrated that the majority of glycolytic enzymes are inherently over-expressed in 70% of human cancers, irrespective of oxygenation (42). Is this cellular overkill and is the elevation of expression for all enzymes in the pathway necessary? Proponents of classical metabolic biochemistry would argue that increased expression of "rate-limiting" enzymes would suffice, or at least be instigated. Ensuring sufficient supply of glucose, or a phosphorylated derivative, would also feature prominently in any strategy to elevate flux through glycolysis. Moreover, tumours display alterations in the isoenzyme expression profile, which may provide isoforms with kinetic properties that can exploit the local environment (1,43,44). The predominant glucose transporter isoforms expressed under hypoxic conditions are GLUT1 and GLUT3; both of which have high affinity for glucose (45). Under standard incubation conditions (i.e. [glucose] ≥ 5mM), transporter activity would be saturated, to ensure efficient influx. Consequently, increasing glucose uptake in hypoxia would require elevated transporter expression, a finding that was observed in the present manuscript.

Contemporary biochemical interpretation of pathways uses Metabolic Control Analysis (MCA), which provide a mathematical framework to describe substrate flux (46,47). This analysis suggests that control of flux through any pathway involves the activities of multiple enzymes. In addition, the model applies elasticity coefficients, which demonstrate the extent to which variation in reactant concentration of any intermediate can change the rate of flux through the pathway. In AS-30D hepatoma cells, the primary control of glycolysis was exerted in the initial stages of the pathway by the glucose transporter and HK activity (48,49). Although PFK1 did exert some control, its influence was considerably lower than GLUT and HK. In the present manuscript, the absolute capacity of PFK1 activity was similar in homogenates from both $TS^N$ and $TS^H$, presumably due to allosteric control by fructose-

2,6-bisphosphate and AMP. Consequently, an increase in the concentration of fructose-6-phosphate is unlikely to confer a significant change in the activity of PFK1. However, the similarity in PFK1 activity and overall glycolytic flux implicate the enzyme as a key control point for this pathway.

MCA based investigations have also suggested prominent roles for GLUT1 and GLUT3 in dictating glycolytic flux, with considerably lower influence by HK under conditions of normal glucose concentration (49). In addition, the transporters retained their influence in cells exposed to hypoxic conditions; although the contribution of PFK1 to glycolytic flux was greater than under normoxia. Figure 4 provides a summary model of the metabolic changes observed in TS exposed to severe hypoxia for a 16 hour period. The $TS^H$ displayed elevated expression of glucose transporters (GLUT1/3) and a corresponding increase in the expression of lactate transporter proteins (MCT1/4). The elevated GLUT proteins will ensure increased glucose uptake from the medium for catabolism via glycolysis. The over-expression of MCT1/4 will promote the clearance of lactate from the cells. This ensures maintenance of a stable intracellular pH and will provide an equilibrium favouring the continued conversion of pyruvate to lactate. In addition, overall activity of PFK1 was maintained in $TS^H$ under severe hypoxia and this was predominantly due to the lack of effect on expression of the PFK-P isoform. Investigations with breast cancer cell lines have demonstrated that PFK1 expression undergoes a gradual conversion to the P-isoform (44,50) and the specific disruption of its expression in glioblastoma provided a survival advantage in a mouse xenograft model (51).

Over-expression of the transporters and retention of PFK1-P expression are therefore likely to promote the enhanced glycolytic flux observed under severe hypoxia. This increased flux occurs under the backdrop of reduced protein expression and/or metabolic capacity for the glycolytic enzymes HK2, PK and LDH. The reduced expression for these enzymes is not correlated with the elevated mRNA levels generated by a strong up-regulation of Hif1α in the $TS^H$. It therefore represents an abridged Hif1α response by the cells to adapt to the severe hypoxia. The metabolic capacities for the enzymes remain in excess of the glycolytic flux, thereby ensuring its progression. It is also pertinent to recall that these three enzymes are also branch points for possible intermediate diversion to biosynthetic pathways. Reduction in their activity/expression may impact on entry to biosynthesis.

The expression of G6PDH protein, the entry point for glucose-6-phosphate to the PPP, was also markedly reduced in severe hypoxia. In addition, the observed reduction in metabolic capacity of this branch-point enzyme ensured that intermediates of glucose catabolism were retained within the glycolytic pathway. Two major roles for the PPP are the provision of NADPH for biosynthetic pathways and ribose sugars that are essential for nucleotide synthesis (52). Therefore, this metabolic shunt has a significant role in cellular anabolic processes. This is in addition to the reduced expression of G6PDH, which is the entry point to the pentose-phosphate pathway and ensures that glycolytic intermediates are not siphoned off to anabolic pathways. As discussed by Hochachka et al (53), the suppression of biosynthetic pathways, and its concomitant reduction in ATP demand, ensures cellular tolerance for hypoxia.

Glutamine has an important role in hypoxic cancer cells as a carbon source for the synthesis of citrate; a major biosynthetic precursor in the synthesis of fatty acids essential for cellular growth and proliferation (54,55). Wise and colleagues employed isotopic tracers in SF188 glioblastoma cells to show that under hypoxic (0.5% $O_2$) conditions sufficient for HIF-1α stabilization, glutamine became the major source of citrate, via a reverse order of TCA cycle reactions where α ketoglutarate from glutaminolysis was reductively carboxylated (55). In addition, HIF-1 activation (0.5% $O_2$) was shown to reduce the activity of the α ketoglutarate dehydrogenase complex, via promotion of the ubiquitination and proteolysis of the E1 subunit of the complex, hence inhibiting glutamine oxidation via the TCA cycle (54). In the present manuscript, expression of the ASCT2 transporter protein mediating glutamine uptake was unaffected by severe hypoxia, whereas expression of GLDH was marginally increased despite a reduction in its metabolic capacity. Taken together, the data suggests a possible small reduction in overall flux through the glutaminolysis pathway. Once again, this appears to reveal a dampening of

biosynthetic pathways in response to severe hypoxia in TS.

A key explanation for the disconnect between mRNA levels and expression of enzymes or transporters is the significant drop in protein synthesis that has been observed in hypoxia. The extent to which protein synthesis is suppressed in cancer cells is time dependent and correlated with oxygen tension (56). In fact, protein synthesis is the second most ATP utilising cellular process, with only the $Na^+/K^+$-ATPase consuming more (53,57). Consequently, suppression of protein synthesis will reduce ATP degradation and thereby "spare" essential cellular survival pathways. Under conditions of severe hypoxia, ATP usage by protein synthesis may drop to 7% of levels observed in normoxia (53). The reduction in protein synthesis in hypoxic cancer cells is attributed to reduced translation. In particular, the reduction in $O_2$ tension results in phosphorylation of the eukaryotic initiation factor (eIF2) and disruption of the eIF4F complex; the combined effects lead to suppression of protein synthesis (58,59).

During the development of hypoxia, cancer cells initiate a series of events to up-regulate glycolytic flux in order to preserve sufficient ATP and biomass for cellular function. The response is co-ordinated primarily by the transcription factor Hif1α and results in elevated mRNA levels for numerous glycolytic enzymes and transporters mediating glucose and lactate translocation. However, under severe hypoxia the increased mRNA levels are not associated with corresponding elevations in protein levels of glycolytic enzymes. This disparity is likely due to a significant reduction in protein synthesis. However, the expression of PFK1-P is maintained and the levels of GLUT1/3 and MCT1/4 are increased. These effects are sufficient to confer an increased glycolytic flux and further reveal the complex balance required in cancer cells to adapt to micro-environmental stresses. In particular, the reduced HK2/PK activities and the unchanged PFK1 capacity would suggest that cellular metabolic strategy in severe hypoxia diverts glucose from biosynthetic pathways to enable sufficient ATP production by glycolysis.

**ACKNOWLEDGEMENTS**

Dr H Smith was funded by a Medical research Council D. Phil. Studentship (10CLS02JOB) awarded by NDCLS to undertake this research in the laboratory of A/Prof Callaghan. AP and JB acknowledge support from Leukaemia and Lymphoma Research UK. MB was supported by a Daphne Jackson Fellowship.

**CONFLICT OF INTEREST**

The authors declare that they have no conflicts of interest with the contents of this article.

**AUTHOR CONTRIBUTIONS**

***HS*** acquired all data sets in the manuscript, analysed the data, facilitated design of the study and assisted in composition of the manuscript. ***MB*** analysed the data, assisted with data collection for Table 1, facilitated design of the study and assisted in composition of the manuscript. ***AP/JB*** designed and assisted with RNA microarray data in Tables 2/3, facilitated analysis of this data and assisted in composition of the manuscript. ***HT*** designed and assisted with histological/IHC data in Figure 1, facilitated analysis of this data and assisted in composition of the manuscript. ***RC*** devised and designed the study, acquired funding to undertake the study, analysed the data, and wrote the manuscript.

**ABBREVIATIONS**

Hif – hypoxia inducible factor
TS – tumour spheroid
GLUT – glucose transporter
MCT – monocarboxylate transporter
ASCT2 – glutamine/amino-acid transporter
HK – hexokinase
PFK – phosphofructokinase

PK – pyruvate kinase
LDH – lactate dehydrogenase
G6PDH – glucose-6-phosphate dehydrogenase
GLDH – glutamate dehydrogenase

**REFERENCES**


1. Ward, P. S., and Thompson, C. B. (2012) Metabolic reprogramming: a cancer hallmark even warburg did not anticipate. *Cancer Cell* **21**, 297-308
2. Moreno-Sanchez, R., Rodriguez-Enriquez, S., Marin-Hernandez, A., and Saavedra, E. (2007) Energy metabolism in tumor cells. *FEBS J* **274**, 1393-1418
3. Bos, R., van Der Hoeven, J. J., van Der Wall, E., van Der Groep, P., van Diest, P. J., Comans, E. F., Joshi, U., Semenza, G. L., Hoekstra, O. S., Lammertsma, A. A., and Molthoff, C. F. (2002) Biologic correlates of (18)fluorodeoxyglucose uptake in human breast cancer measured by positron emission tomography. *J Clin Oncol* **20**, 379-387
4. DeBerardinis, R. J., Lum, J. J., Hatzivassiliou, G., and Thompson, C. B. (2008) The biology of cancer: metabolic reprogramming fuels cell growth and proliferation. *Cell Metab* **7**, 11-20
5. Soga, T. (2013) Cancer metabolism: key players in metabolic reprogramming. *Cancer Sci* **104**, 275-281
6. Morrish, F., Isern, N., Sadilek, M., Jeffrey, M., and Hockenbery, D. M. (2009) c-Myc activates multiple metabolic networks to generate substrates for cell-cycle entry. *Oncogene* **28**, 2485-2491
7. Dang, C. V., Le, A., and Gao, P. (2009) MYC-induced cancer cell energy metabolism and therapeutic opportunities. *Clin Cancer Res* **15**, 6479-6483
8. Osthus, R. C., Shim, H., Kim, S., Li, Q., Reddy, R., Mukherjee, M., Xu, Y., Wonsey, D., Lee, L. A., and Dang, C. V. (2000) Deregulation of glucose transporter 1 and glycolytic gene expression by c-Myc. *J Biol Chem* **275**, 21797-21800
9. Shim, H., Dolde, C., Lewis, B. C., Wu, C. S., Dang, G., Jungmann, R. A., Dalla-Favera, R., and Dang, C. V. (1997) c-Myc transactivation of LDH-A: implications for tumor metabolism and growth. *Proc Natl Acad Sci U S A* **94**, 6658-6663
10. Zeng, W., Liu, P., Pan, W., Singh, S. R., and Wei, Y. (2015) Hypoxia and hypoxia inducible factors in tumor metabolism. *Cancer Lett* **356**, 263-267
11. Schwartzenberg-Bar-Yoseph, F., Armoni, M., and Karnieli, E. (2004) The tumor suppressor p53 down-regulates glucose transporters GLUT1 and GLUT4 gene expression. *Cancer Res* **64**, 2627-2633
12. Mazurek, S. (2011) Pyruvate kinase type M2: a key regulator of the metabolic budget system in tumor cells. *Int J Biochem Cell Biol* **43**, 969-980
13. van Berkel, J. C. (1974) Some kinetic properties of M2-type pyruvate kinase from rat liver at physiological Mg2+ concentration. *Biochim Biophys Acta* **370**, 140-152
14. Krogh, A. (1919) The number and distribution of capillaries in muscles with calculations of the oxygen pressure head necessary for supplying the tissue. *J Physiol* **52**, 409-415
15. Grimes, D. R., Kelly, C., Bloch, K., and Partridge, M. (2014) A method for estimating the oxygen consumption rate in multicellular tumour spheroids. *J R Soc Interface* **11**, 20131124
16. Dewhirst, M. W., Secomb, T. W., Ong, E. T., Hsu, R., and Gross, J. F. (1994) Determination of local oxygen consumption rates in tumors. *Cancer Res* **54**, 3333-3336
17. Helmlinger, G., Yuan, F., Dellian, M., and Jain, R. K. (1997) Interstitial pH and pO2 gradients in solid tumors in vivo: high-resolution measurements reveal a lack of correlation. *Nat Med* **3**, 177-182
18. Heldin, C. H., Rubin, K., Pietras, K., and Ostman, A. (2004) High interstitial fluid pressure - an obstacle in cancer therapy. *Nat Rev Cancer* **4**, 806-813
19. Stohrer, M., Boucher, Y., Stangassinger, M., and Jain, R. K. (2000) Oncotic pressure in solid tumors is elevated. *Cancer Res* **60**, 4251-4255
20. Brahimi-Horn, M. C., Chiche, J., and Pouyssegur, J. (2007) Hypoxia signalling controls metabolic demand. *Curr Opin Cell Biol* **19**, 223-229

21. Salceda, S., and Caro, J. (1997) Hypoxia-inducible factor 1alpha (HIF-1alpha) protein is rapidly degraded by the ubiquitin-proteasome system under normoxic conditions. Its stabilization by hypoxia depends on redox-induced changes. *J Biol Chem* **272**, 22642-22647
22. Kress, S., Stein, A., Maurer, P., Weber, B., Reichert, J., Buchmann, A., Huppert, P., and Schwarz, M. (1998) Expression of hypoxia-inducible genes in tumor cells. *J Cancer Res Clin Oncol* **124**, 315-320
23. Dhani, N., Fyles, A., Hedley, D., and Milosevic, M. (2015) The clinical significance of hypoxia in human cancers. *Semin Nucl Med* **45**, 110-121
24. Walsh, J. C., Lebedev, A., Aten, E., Madsen, K., Marciano, L., and Kolb, H. C. (2014) The clinical importance of assessing tumor hypoxia: relationship of tumor hypoxia to prognosis and therapeutic opportunities. *Antioxid Redox Signal* **21**, 1516-1554
25. Bertout, J. A., Patel, S. A., and Simon, M. C. (2008) The impact of O2 availability on human cancer. *Nat Rev Cancer* **8**, 967-975
26. Koong, A. C., Mehta, V. K., Le, Q. T., Fisher, G. A., Terris, D. J., Brown, J. M., Bastidas, A. J., and Vierra, M. (2000) Pancreatic tumors show high levels of hypoxia. *Int J Radiat Oncol Biol Phys* **48**, 919-922
27. Dunst, J., Stadler, P., Becker, A., Lautenschlager, C., Pelz, T., Hansgen, G., Molls, M., and Kuhnt, T. (2003) Tumor volume and tumor hypoxia in head and neck cancers. The amount of the hypoxic volume is important. *Strahlenther Onkol* **179**, 521-526
28. Nordsmark, M., Overgaard, M., and Overgaard, J. (1996) Pretreatment oxygenation predicts radiation response in advanced squamous cell carcinoma of the head and neck. *Radiother Oncol* **41**, 31-39
29. Movsas, B., Chapman, J. D., Horwitz, E. M., Pinover, W. H., Greenberg, R. E., Hanlon, A. L., Iyer, R., and Hanks, G. E. (1999) Hypoxic regions exist in human prostate carcinoma. *Urology* **53**, 11-18
30. Hall, M. D., Martin, C., Ferguson, D. J. P., Phillips, R. M., Hambley, T. W., and Callaghan, R. (2004) Comparative efficacy of novel platinum(IV) compounds with established chemotherapeutic drugs in solid tumour models. *Biochemical Pharmacology* **67**, 17-30
31. Mellor, H. R., Ferguson, D. J. P., and Callaghan, R. (2005) A model of quiescent tumour microregions for evaluating multicellular resistance to chemotherapeutic drugs. *British Journal of Cancer* **93**, 302-309
32. Mellor, H. R., Snelling, S., Hall, M. D., Modok, S., Jaffar, M., Hambley, T. W., and Callaghan, R. (2005) The influence of tumour microenvironmental factors on the efficacy of cisplatin and novel platinum(IV) complexes. *Biochem Pharmacol* **70**, 1137-1146
33. Bloch, K., Smith, H., van Hamel Parsons, V., Gavaghan, D., Kelly, C., Fletcher, A., Maini, P., and Callaghan, R. (2014) Metabolic alterations during the growth of tumour spheroids. *Cell Biochem Biophys* **68**, 615-628
34. Board, M., Humm, S., and Newsholme, E. A. (1990) Maximum activities of key enzymes of glycolysis, glutaminolysis, pentose phosphate pathway and tricarboxylic acid cycle in normal, neoplastic and suppressed cells. *Biochem J* **265**, 503-509
35. Brown, D., and Garratt, C. J. (1974) A simple method for determining total glucose utilisation by isolated adipocytes using (5-3H)-glucose. *Anal Biochem* **61**, 492-499
36. Pellagatti, A., Cazzola, M., Giagounidis, A., Perry, J., Malcovati, L., Della Porta, M. G., Jadersten, M., Killick, S., Verma, A., Norbury, C. J., Hellstrom-Lindberg, E., Wainscoat, J. S., and Boultwood, J. (2010) Deregulated gene expression pathways in myelodysplastic syndrome hematopoietic stem cells. *Leukemia* **24**, 756-764
37. Farmer, S. R., Wan, K. M., Ben-Ze'ev, A., and Penman, S. (1983) Regulation of actin mRNA levels and translation responds to changes in cell configuration. *Mol Cell Biol* **3**, 182-189
38. Sutherland, R. M. (1988) Cell and environment interactions in tumor microregions: the multicell spheroid model. *Science* **240**, 177-184
39. Dang, C. V., Kim, J. W., Gao, P., and Yustein, J. (2008) The interplay between MYC and HIF in cancer. *Nat Rev Cancer* **8**, 51-56
40. Christofk, H. R., Vander Heiden, M. G., Harris, M. H., Ramanathan, A., Gerszten, R. E., Wei, R., Fleming, M. D., Schreiber, S. L., and Cantley, L. C. (2008) The M2 splice isoform of pyruvate kinase is important for cancer metabolism and tumour growth. *Nature* **452**, 230-233

41. Thoma, C. R., Zimmermann, M., Agarkova, I., Kelm, J. M., and Krek, W. (2014) 3D cell culture systems modeling tumor growth determinants in cancer target discovery. *Adv Drug Deliv Rev* **69-70**, 29-41
42. Altenberg, B., and Greulich, K. O. (2004) Genes of glycolysis are ubiquitously overexpressed in 24 cancer classes. *Genomics* **84**, 1014-1020
43. Chen, J. Q., and Russo, J. (2012) Dysregulation of glucose transport, glycolysis, TCA cycle and glutaminolysis by oncogenes and tumor suppressors in cancer cells. *Biochim Biophys Acta* **1826**, 370-384
44. Wang, G., Xu, Z., Wang, C., Yao, F., Li, J., Chen, C., and Sun, S. (2013) Differential phosphofructokinase-1 isoenzyme patterns associated with glycolytic efficiency in human breast cancer and paracancer tissues. *Oncol Lett* **6**, 1701-1706
45. Gould, G. W., and Holman, G. D. (1993) The glucose transporter family: structure, function and tissue-specific expression. *Biochem J* **295 ( Pt 2)**, 329-341
46. Moreno-Sanchez, R., Saavedra, E., Rodriguez-Enriquez, S., and Olin-Sandoval, V. (2008) Metabolic control analysis: a tool for designing strategies to manipulate metabolic pathways. *J Biomed Biotechnol* **2008**, 597913
47. TeSlaa, T., and Teitell, M. A. (2014) Techniques to monitor glycolysis. *Methods Enzymol* **542**, 91-114
48. Marin-Hernandez, A., Gallardo-Perez, J. C., Rodriguez-Enriquez, S., Encalada, R., Moreno-Sanchez, R., and Saavedra, E. (2011) Modeling cancer glycolysis. *Biochim Biophys Acta* **1807**, 755-767
49. Rodriguez-Enriquez, S., Marin-Hernandez, A., Gallardo-Perez, J. C., and Moreno-Sanchez, R. (2009) Kinetics of transport and phosphorylation of glucose in cancer cells. *J Cell Physiol* **221**, 552-559
50. Moon, J. S., Kim, H. E., Koh, E., Park, S. H., Jin, W. J., Park, B. W., Park, S. W., and Kim, K. S. (2011) Kruppel-like factor 4 (KLF4) activates the transcription of the gene for the platelet isoform of phosphofructokinase (PFKP) in breast cancer. *J Biol Chem* **286**, 23808-23816
51. Sanzey, M., Abdul Rahim, S. A., Oudin, A., Dirkse, A., Kaoma, T., Vallar, L., Herold-Mende, C., Bjerkvig, R., Golebiewska, A., and Niclou, S. P. (2015) Comprehensive analysis of glycolytic enzymes as therapeutic targets in the treatment of glioblastoma. *PLoS One* **10**, e0123544
52. Jiang, P., Du, W., Wang, X., Mancuso, A., Gao, X., Wu, M., and Yang, X. (2011) p53 regulates biosynthesis through direct inactivation of glucose-6-phosphate dehydrogenase. *Nat Cell Biol* **13**, 310-316
53. Hochachka, P. W., Buck, L. T., Doll, C. J., and Land, S. C. (1996) Unifying theory of hypoxia tolerance: molecular/metabolic defense and rescue mechanisms for surviving oxygen lack. *Proc Natl Acad Sci U S A* **93**, 9493-9498
54. Sun, R. C., and Denko, N. C. (2014) Hypoxic regulation of glutamine metabolism through HIF1 and SIAH2 supports lipid synthesis that is necessary for tumor growth. *Cell Metab* **19**, 285-292
55. Wise, D. R., Ward, P. S., Shay, J. E., Cross, J. R., Gruber, J. J., Sachdeva, U. M., Platt, J. M., DeMatteo, R. G., Simon, M. C., and Thompson, C. B. (2011) Hypoxia promotes isocitrate dehydrogenase-dependent carboxylation of alpha-ketoglutarate to citrate to support cell growth and viability. *Proc Natl Acad Sci U S A* **108**, 19611-19616
56. Sorensen, B. S., Hao, J., Overgaard, J., Vorum, H., Honore, B., Alsner, J., and Horsman, M. R. (2005) Influence of oxygen concentration and pH on expression of hypoxia induced genes. *Radiother Oncol* **76**, 187-193
57. Buck, L. T., and Hochachka, P. W. (1993) Anoxic suppression of Na(+)-K(+)-ATPase and constant membrane potential in hepatocytes: support for channel arrest. *Am J Physiol* **265**, R1020-1025
58. Hernandez-Jimenez, M., Ayuso, M. I., Perez-Morgado, M. I., Garcia-Recio, E. M., Alcazar, A., Martin, M. E., and Gonzalez, V. M. (2012) eIF4F complex disruption causes protein synthesis inhibition during hypoxia in nerve growth factor (NGF)-differentiated PC12 cells. *Biochim Biophys Acta* **1823**, 430-438

59. Koumenis, C., Naczki, C., Koritzinsky, M., Rastani, S., Diehl, A., Sonenberg, N., Koromilas, A., and Wouters, B. G. (2002) Regulation of protein synthesis by hypoxia via activation of the endoplasmic reticulum kinase PERK and phosphorylation of the translation initiation factor eIF2alpha. *Mol Cell Biol* **22**, 7405-7416

## FIGURE LEGENDS

**Figure 1 Effects of severe hypoxia on the tumour spheroid expression of markers for proliferation, quiescence and hypoxia**

Markers of proliferation (Ki67), quiescence ($p27^{Kip1}$) and hypoxia (pimonidazole) were measured using immunohistochemistry. Tumour spheroids were fixed in formalin and embedded in wax moulds. Sections (5µm) were cut and markers identified as described in materials and methods. Sections were counterstained with haematoxylin and mounted to slides with AquaMount. The scale bar corresponds to 200 µm. Panels (a-b) were stained for pimonidazole, (c-d) stained for Ki67 and (e-f) for $p27^{Kip1}$. Panels (a,c,e) were obtained from spheroids grown in normoxic conditions and (b,d,f) from hypoxic conditions.

**Figure 2 Cellular outgrowth from tumour spheroids following growth in conditions of severe hypoxia**

Tumour spheroids were grown at 37ºC under normoxic conditions ($pO_2$~20%, $pCO_2$~5%) or subjected to severe hypoxia ($pO_2$~0.1%) for 16 hours. Following incubation, the spheroids were transferred to uncoated 96-well plates and incubated for a further 72 hours under standard, normoxic conditions. Panel (a) shows a photomicrograph of a representative spheroid and the cellular outgrowth. Cells were stained with methylene blue. The radii of the spheroid and the cellular outgrowth were measured using a graduated eyepiece graticule. Panel (b) shows the mean±sem (n=20) of the radius of outgrowth from spheroids that had been grown under normoxic (*empty bar*) or hypoxic (*filled bar*) conditions. The radius of the normoxic spheroids was assigned a value of 1.0.

**Figure 3 Expression of the transcription factors Hif1α and c-Myc in tumour spheroids following growth in conditions of severe hypoxia**

Expression of the transcription factors (a) Hif1α and (b) c-Myc were determined for tumour spheroids grown under conditions of normoxia ($TS^N$) or severe hypoxia ($TS^H$). The inset to each panel shows a representative western immunoblot of spheroid lysate detected as described in the materials and methods. Equivalent loading between samples was achieved by using 10µg total protein per lane. Densitometric analysis was used to quantify the expression with the level in $TS^N$ assigned a value of 1.0. Values represent mean±sem from at least four independent preparations. * indicates a statistically significant ($p<0.001$) difference to the $TS^N$ level.

**Figure 4 Metabolic alterations in response to severe hypoxia in tumour spheroids**

The figure provides a schematic representation of the effects of severe hypoxia on the fate and flux of glucose. Arrows represent transport processes or metabolic reactions. The solid arrows highlight those processes similar, or increased from that observed in normoxia. The dashed lines indicate that flux through the specific reaction/transfer has been reduced. The blue boxes refer to transporters and enzymes investigated in this study. Solid boxes indicate that expression has been elevated compared to normoxia and the dashed boxes indicate reduced expression.

**TABLES**

| | **$TS^N$ FLUX** | **$TS^H$ FLUX** |
|---|---|---|
| **Glycolytic flux** ($\mu mol\ mg^{-1}\ min^{-1}$) | 19.3±1.7 | 37.8±3.2 |
| *(n)* | *(4)* | *(4)* |
| P | | <0.001 |

**Table 1 The effects of severe hypoxia on the glycolytic flux rate in tumour spheroids**
The glycolytic flux was determined from the rate of tritium removal from D-[5-$^3$H(N)]-glucose added to spheroids grown under normoxic conditions ($pO_2$~20%, $pCO_2$~5%) or subjected to severe hypoxia ($pO_2$~0.1%) for 16 hours. The radiolabelled glucose was added to intact spheroids and the rate corresponds to µmoles [$^3$H] removed from D-[5-$^3$H(N)]-glucose per mg total spheroid protein per min. Values correspond to mean±sem from the number of independent preparations indicated in parentheses.

| TRANSPORTER | ISOFORM | EXPRESSION RATIO ($TS^H/TS^N$) | |
|---|---|---|---|
| | | mRNA | Protein |
| Glucose transporter 1 (GLUT1) | SLC2A1 | 2.7 | 1.53±0.19 *(4)* |
| Glucose transporter 3 (GLUT3) | SLC2A3 | 8.2 | 1.96±0.17* *(7)* |
| Monocarboxylate transporter 1 (MCT1) | SLC16A1 | 0.66 | 1.51±0.16* *(5)* |
| Monocarboxylate transporter 4 (MCT4) | SLC16A3 | 1.1 | 1.51±0.09* *(7)* |
| Glutamine transporter (ASCT2) | SLC1A5 | 0.79 | 1.18±0.28 *(9)* |

**Table 2 The effects of severe hypoxia on the expression profiles of transporters associated with cellular metabolism**

Tumour spheroids were subjected to severe hypoxia (þ$O_2$~0.1%) for 16 hours at 37ºC. Following hypoxic incubation, the spheroids were prepared for analysis of transporter expression. mRNA data for the expression of metabolism associated transporters were determined using gene expression profiling. Protein expression levels were determined by Western Blot analysis of total protein homogenates (10µg). Densitometric analysis was used to quantify the relative levels of protein from spheroids grown under normoxic or hypoxic conditions. Expression of protein and mRNA was normalised to the level found in normoxic spheroids, which were assigned a value of 1.0. The mRNA levels were obtained from a pooled sample from three spheroid preparations. The protein levels represent the mean±sem obtained from the number of independent samples indicated by the value in parentheses.* signifies a statistically significant difference to the normoxic condition ($p<0.01$).

| **ENZYME** | **ISOFORM** | **EXPRESSION RATIO** ($TS^H/TS^N$) | | **MAXIMAL ACTIVITY** (*nmoles* $min^{-1}$ $mg^{-1}$) | |
|---|---|---|---|---|---|
| | | mRNA | Protein | Normoxic | Hypoxic |
| Hexokinase | HK2 | 2.37 | 0.17±0.07 *(11)* | 6.26±1.02 *(11)* | 1.33±0.29 *(4)* |
| Phosphofructokinase1 | PFK1-P | - | 0.89±0.49 *(3)* | 29.6±9.9 *(4)* | 31.9±6.9 *(4)* |
| | PFK1-M | 0.80 | 0.30±0.11 *(16)* | | |
| | PFK1-L | 1.42 | 0.16±0.11 *(7)* | | |
| Pyruvate kinase | PK | 1.53 | 0.25±0.09 *(8)* | 2155±258 *(5)* | 545±311 *(4)* |
| Lactate dehydrogenase | LDH | 1.71 | 0.29±0.09 *(10)* | 1305±231 *(5)* | 384±154 *(4)* |
| Glucose-6-phosphate dehydrogenase | G6P-DH | 1.03 | 0.09±004 *(6)* | 184±17 *(5)* | 32±12 *(4)* |
| Glutamate dehydrogenase | GLDH | - | 1.61±0.27 *(8)* | 22.9±2.3 *(4)* | 4.4±3.0 *(4)* |

**Table 3 The effects of severe hypoxia on the expression profiles of cytosolic enzymes associated with cellular metabolism**

Tumour spheroids were grown at 37$^{o}$C under normoxic conditions ($pO_2$~20%, $pCO_2$~5%) or subjected to severe hypoxia ($pO_2$~0.1%) for 16 hours. mRNA data for the expression of metabolism associated enzymes were determined using gene expression profiling. Protein expression levels were determined by Western Blot analysis of total protein homogenates (10µg). Expression of protein and mRNA was normalised to the level found in normoxic spheroids, which were assigned a value of 1.0. Activities of were measured from spheroid homogenates under conditions of high substrate concentration to provide the maximal enzyme activity. All activities represent mean±sem from the number of independent preparations indicated in parentheses and in units of nmoles substrate consumed per mg total protein per minute.

**FIGURES**

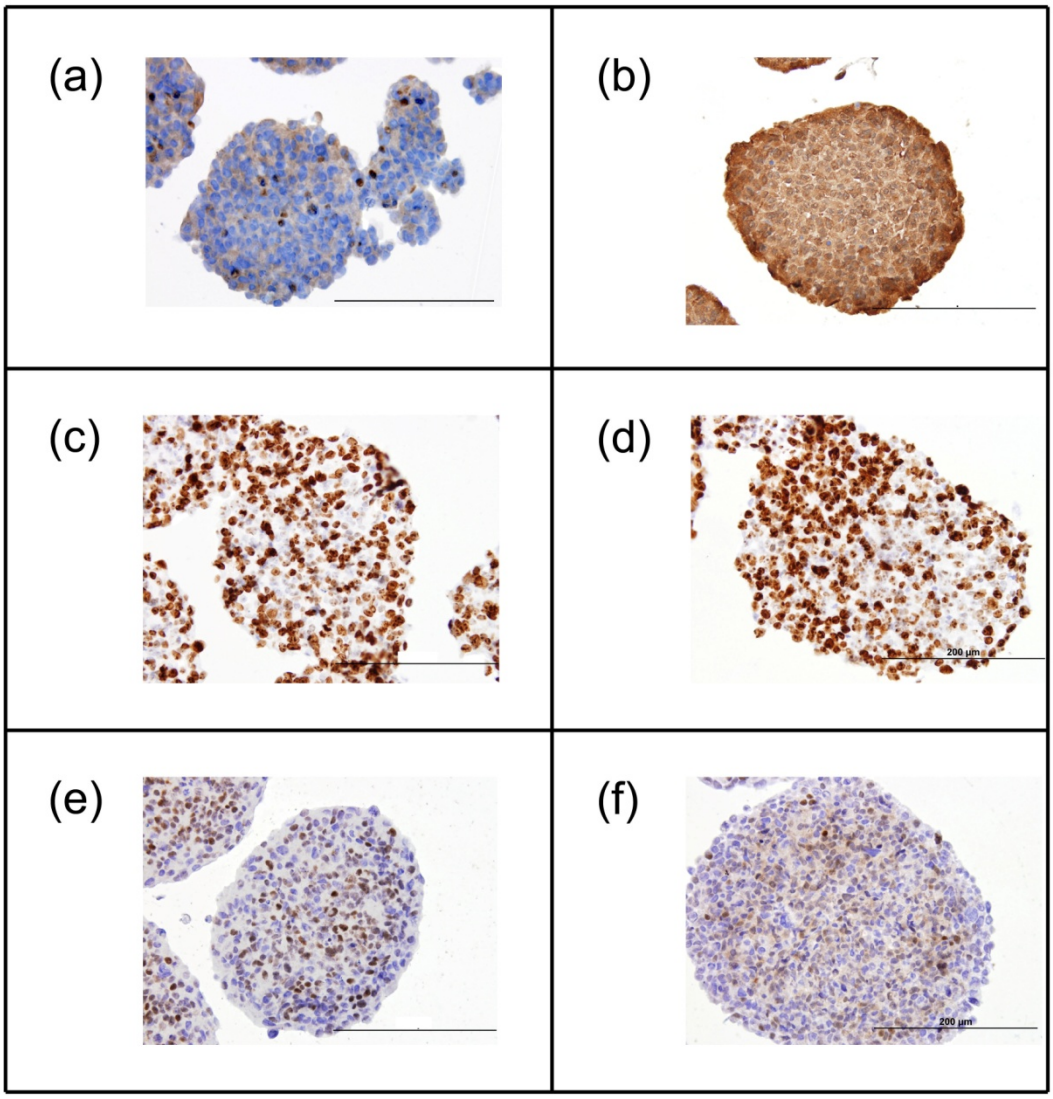


Figure 1

(a)

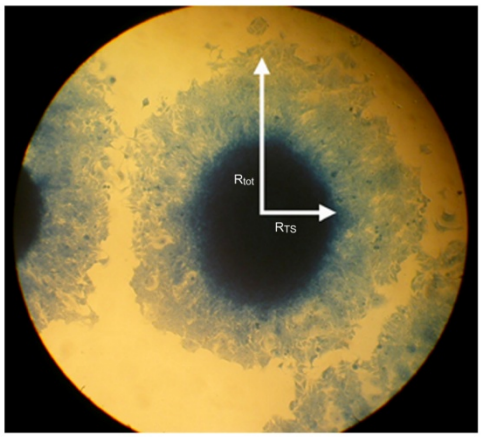


(b)

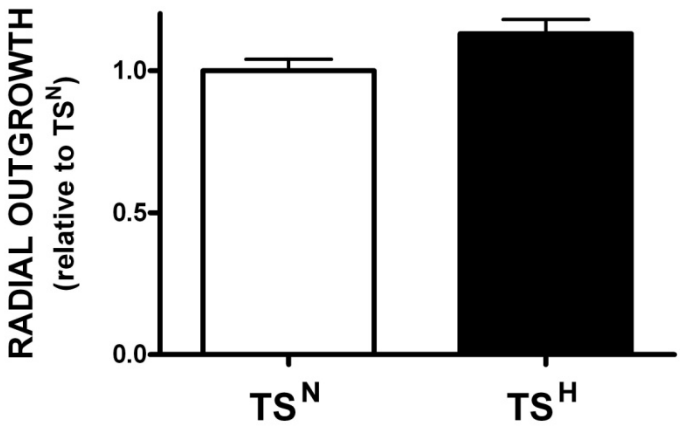


Figure 2

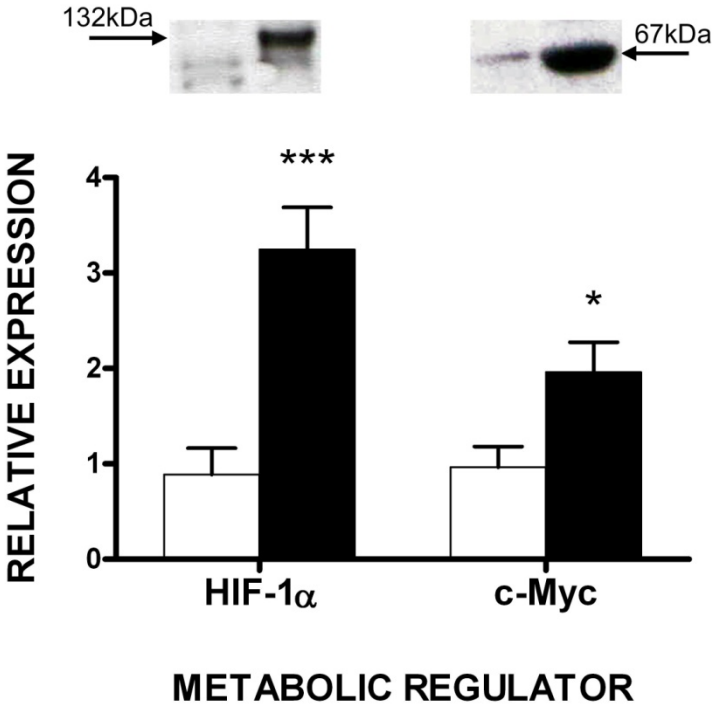
132kDa
67kDa
RELATIVE EXPRESSION
4
3
2
1
0
***
*
HIF-1α
c-Myc
METABOLIC REGULATOR

Figure 3

Figure 4

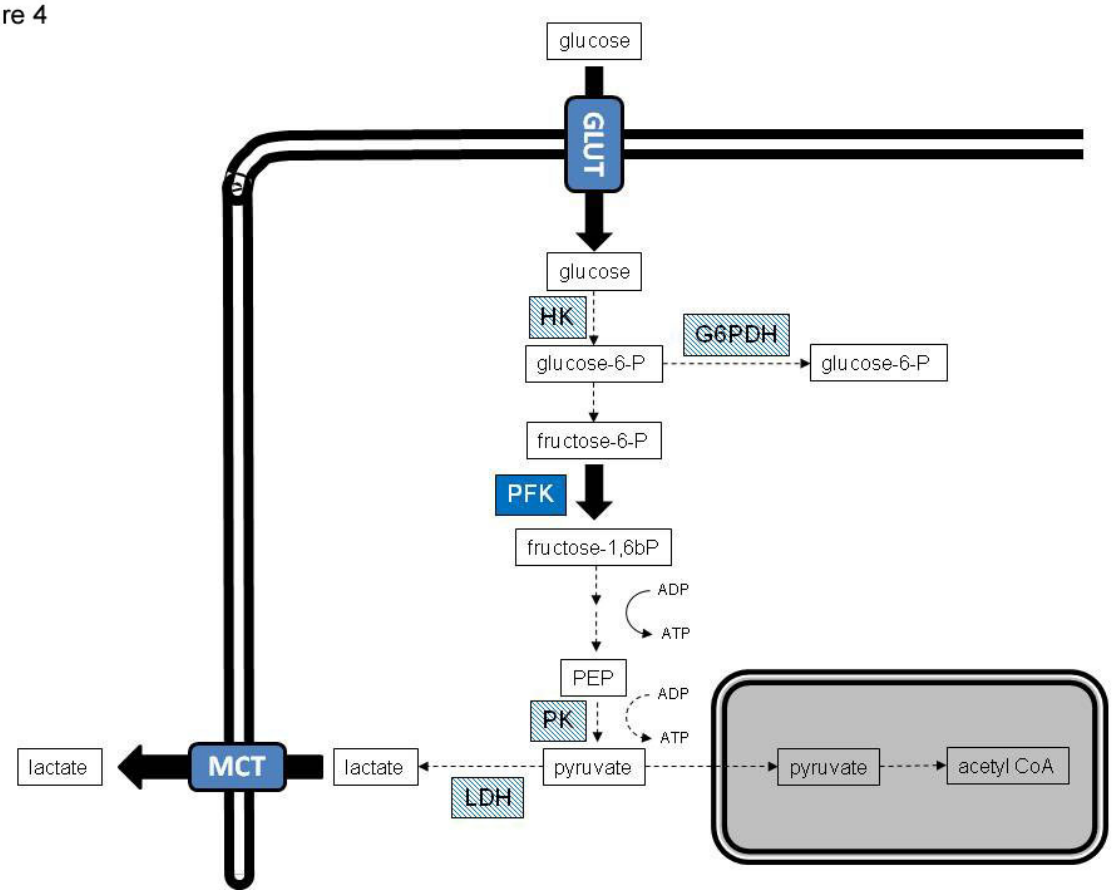
glucose
GLUT
glucose
HK
G6PDH
glucose-6-P
glucose-6-P
fructose-6-P
PFK
fructose-1,6bP
ADP
ATP
PEP
ADP
PK
ATP
lactate
MCT
lactate
pyruvate
pyruvate
acetyl CoA
LDH